

# A Two Mobilized-Plane Model for Soil Liquefaction Analysis

## 액상화해석을 위한 두 개의 활성화면을 가진 구성모델

Park, Sung-Sik<sup>1</sup> 박 성 식

### 요 지

본 논문에서는 정적 및 액상화와 같은 동적하중을 받는 흙의 거동해석을 위한 두 개의 활성화면을 가진 구성모델을 제안하였다. 이 모델은 두 개의 활성화면에 기초하고 있으며, 첫번째면은 회전하는 최대전단면을 나타내며 두번째면은 고정된 수평면을 나타낸다. 이와 같은 두 개의 활성화면을 이용하여 본 모델은 초기의 다른 응력상태하에 있는 시료의 직접단순전단시에 발생하는 주응력회전현상을 모델링할 수 있다. 제안된 모델은 초기의 응력비에 관계없이 평균유효응력이 동일할 경우에 유사한 거동을 보이는 흙의 실내실험결과를 묘사할 수 있다. 그리고, 배수시 반복 직접단순전단으로 발생하는 흙의 거동 즉 제하시에 나타나는 체적감소 및 대변형에서 발생하는 체적팽창을 묘사할 수 있다. 비배수시의 흙의 정적 및 동적 거동은 배수거동에서 흙 골격사이에 존재하는 물의 구속력을 고려함으로써 해석하였다. 본 모델의 구성관계식은 응력-물의 상관관계를 동시에 묘사할 수 있는 FLAC을 이용하여 구현하였다. 배수 직접단순전단 시험을 이용한 Fraser River Sand의 실험결과를 이용하여 모델을 먼저 검증하였으며, 동일한 입력변수를 이용한 Fraser River Sand 비배수 거동의 예측치와 실험치를 비교하여 검증하였다.

### Abstract

A Two Mobilized-Plane Model is proposed for monotonic and cyclic soil response including liquefaction. This model is based on two mobilized planes: a plane of maximum shear stress, which rotates, and a horizontal plane which is spatially fixed. By controlling two mobilized planes, the model can simulate the principal stress rotation effect associated with simple shear from different  $K_0$  states. The proposed model gives a similar skeleton behaviour for soils having the same mean stress, regardless of  $K_0$  conditions as observed in laboratory tests. The soil skeleton behaviour observed in cyclic drained simple shear tests, including compaction during unloading and dilation at large strain is captured in the model. Undrained monotonic and cyclic response is predicted by imposing the volumetric constraint of the water on the drained or skeleton behaviour. This constitutive model is incorporated into the dynamic coupled stress-flow finite difference program of FLAC (Fast Lagrangian Analysis of Continua). The model was first calibrated with drained simple shear tests on Fraser River sand, and verified by comparing predicted and measured undrained behaviour of Fraser River sand using the same input parameters.

**Keywords :** Principal stress rotation, Simple shear test, Two mobilized planes

### 1. Introduction

The effect of principal stress rotation significantly

influences soil behaviour and has received substantial attention since Arthur et al. (1980). A few different types of numerical models considering principal stress rotation

<sup>1</sup> 정회원, 경북대학교 공과대학 토목공학과 (Member, Post-Doctoral Researcher, Dept. of Civil Engrg., Kyungpook National Univ., park1059@hanmail.net)

\* 본 논문에 대한 토의를 원하는 회원은 2007년 4월 30일까지 그 내용을 학회로 보내주시기 바랍니다. 저자의 검토 내용과 함께 논문집에 게재하여 드립니다.

effects have been proposed. These are mainly based on plasticity. One of them is a multi-laminate model proposed by Pande and Sharma (1983). Recently, Lee and Pande (2004) presented its extension to soil liquefaction analysis. This model was originally proposed to study rock joint behaviour by considering many slip planes. Alternatively, Matsuoka (1974) proposed a similar idea but a different concept called multimechanism that used only a maximum obliquity plane,  $45+\phi/2$  for three different shearing mechanisms. Each shearing mechanism is based on two of three principal stresses (i.e.  $\sigma'_1$  and  $\sigma'_2$ ,  $\sigma'_2$  and  $\sigma'_3$ ,  $\sigma'_3$  and  $\sigma'_1$ ). Kabilamany and Ishihara (1991) also proposed a similar concept in three dimensional stress space. In their models, plastic strains from three mechanisms are independently produced and superimposed. The practicality of utilizing such numerical models depends on their simplicity and robustness (Kolymbas 2000). This is particularly so for dynamic analyses. Consequently, the practical application of models for dynamic analyses has been limited to few cases.

A plasticity based constitutive model has been developed at the University of British Columbia (UBC) to handle plastic unloading and principal stress rotation associated with anisotropic consolidation, or  $K_0$  state and is presented here. The proposed model uses two mobilized planes, a maximum shear stress plane which rotates as the direction of the principal stress rotates, and a horizontal plane which is spatially fixed. Under simple shear conditions the plane of maximum shear is initially at 45 degrees to the horizontal and as the shear stress is applied the plane rotates and becomes nearly horizontal at failure. This concept is therefore referred to as a Two Mobilized-Plane Model. The characteristics of this model and its formulation are introduced, and a comparison with laboratory data is presented.

## 2. Simple Shear Behaviour Under Isotropic and $K_0$ Conditions and its Modelling

Rotation of principal stresses occurs in simple shear loading and its effect depends very much on the initial  $K_0$  consolidation state. If  $K_0 = 1.0$ , then as soon as any

horizontal shear stress is applied, the horizontal plane becomes the plane of maximum shear and essentially remains so for the rest of the loading. For this case the plane of maximum shear is horizontal for the duration of loading, and there is no rotation effect. Classical plasticity with a single rotating plane of maximum shear simulates this condition very well. If  $K_0 = 0.5$ , then a large shear stress acts on the 45 degree plane. As the horizontal shear stress is applied, the plane of maximum shear gradually rotates and becomes approximately horizontal at failure (Roscoe 1970). Thus, there is a gradual rotation of principal stress during the loading process. A classical plasticity approach with a single plane cannot capture the observed response in this case. The author has found that the observed response can be captured by adding a plastic contribution from the horizontal plane.

From drained monotonic torsional tests using hollow cylindrical samples, Wijewickreme and Vaid (2004) found that the shear stress-shear strain behaviour on a horizontal plane under the same mean stress is independent of stress path at small strain ranges (shear strain  $\gamma < 0.5\%$ ) for loose sand. In simple shear, this finding can infer that shear stress-strain behaviour of loose sands is the same at small strain level regardless of  $K_0$  state as long as initial mean stresses are the same.

Ishihara (1996) showed that  $K_0$  has a significant effect on liquefaction resistance of sands based on a series of torsional tests with lateral confinement. He found that the cyclic resistance ratio,  $\tau/\sigma'_{v0}$  where  $\sigma'_{v0}$  is the initial vertical effective stress, under  $K_0 = 1.0$  condition is stiffer and stronger than that observed under  $K_0 = 0.5$  condition. On the other hand, there was no significant difference between the  $K_0 = 1.0$  and 0.5 conditions when the cyclic resistance was examined in terms of  $\tau/\sigma'_{m0}$  where  $\sigma'_{m0}$  is the initial mean effective stress. Iai et al. (1992) considered  $K_0$  consolidated elements using a generalized plasticity approach. They mentioned that conventional plasticity models cannot simulate  $K_0 = 0.5$  simple shear tests because they involve effects of rotation of principal stress. The proposed plasticity model can simulate rotation effects associated with  $K_0$  simple shear loading by incorporating two mobilized planes rather

than one. Numerical simulations under two  $K_0$  conditions, 0.5 and 1.0, are compared with measured liquefaction behaviour.

The proposed model referred to as a Two Mobilized-Plane Model is an extension of a simpler model called UBCSAND to include plastic unloading and rotation of principal planes associated with simple shear loading. UBCSAND originally considered unloading as elastic. From a practical point of view, elastic unloading may be adequate for preliminary analysis. However, laboratory data indicate that significant plastic deformation always occurs during the unloading phase. Plastic unloading is particularly important following a large stress cycle that has induced dilation. In the proposed constitutive model, plastic unloading is incorporated by mobilizing plastic deformation on a horizontal plane.

### 3. Two Mobilized-Plane Model: UBCSAND2

The UBCSAND modifies the Mohr-Coulomb model incorporated in FLAC (Fast Lagrangian Analysis of Continua) Version 4.0 (Itasca 2000) to incorporate the plastic strains that occur at all stages of loading. This model has been substantially improved to better model observing sand behaviour and includes the effects of rotation of principal planes or  $K_0$  effect, and plastic unloading as mentioned earlier. These two factors recently incorporated into the Two Mobilized-Plane Model are presented in this paper. The concept and formulations of this model are described in this section including plastic deformations mobilized on two planes.

#### 3.1 Concept of Two Mobilized-Plane Model

The concept of Two Mobilized-Plane Model (called UBCSAND2) is described here. Shear stress increments on two planes causing plastic strains are illustrated in Figure 1 for simple shear conditions with  $K_0 = 0.5$ . Figure 1 (a) represents conditions at the start of shearing when  $\tau_{xy} = 0$  and a small increment  $\Delta\tau_{xy}$  is applied. In this case the plane of maximum shear is at 45 degrees ( $\beta = 45^\circ$ ) as illustrated in Figures 1 (a) and 2 (a), and

while there is a large shear stress from the  $K_0$  condition, the increments of shear and normal stresses  $\Delta\tau$  and  $\Delta\sigma$  on this plane are both zero, and hence no plastic strains are predicted. This results in an initial very stiff elastic response from classical plasticity based on a single plane. However, the stress increment on the horizontal plane,  $\Delta\tau_{xy}$  will cause plastic strains on the horizontal plane and all other planes except for the 45 plane. When this second plane is considered, a much softer response is predicted as shown in Figure 3, condition A.

A later stage of loading is depicted in Figure 1 (b). Here  $\tau_{xy}$  is approaching its failure value and the plane of maximum shear has swung around to become nearly horizontal as illustrated in Figures 1 (b) and 2 (b). Now the  $\Delta\tau \approx \Delta\tau_{xy}$  and both planes essentially coincide. Consideration of both planes would essentially predict double

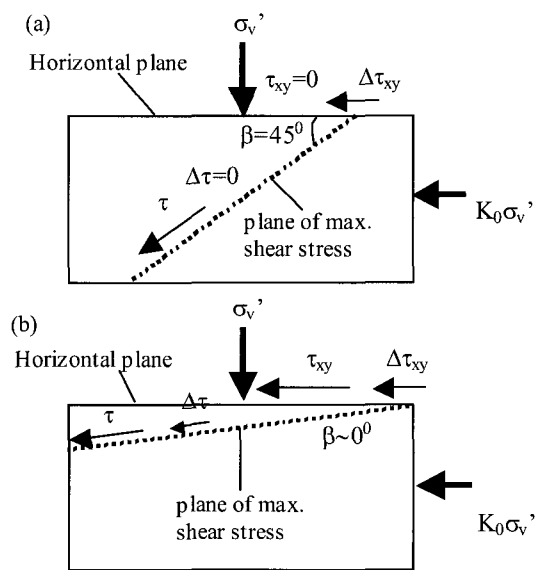


Fig. 1. Stress conditions on two mobilized planes: (a) at small strain level and (b) at large strain level

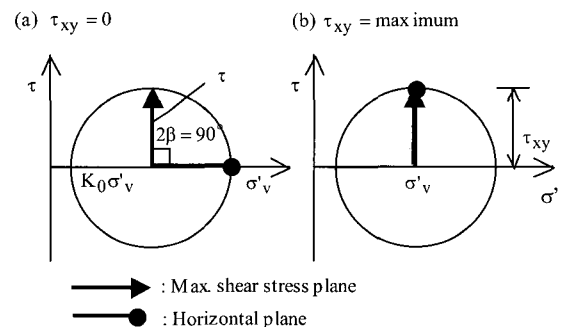


Fig. 2. Rotation of the plane of maximum shear stress under  $K_0$  condition

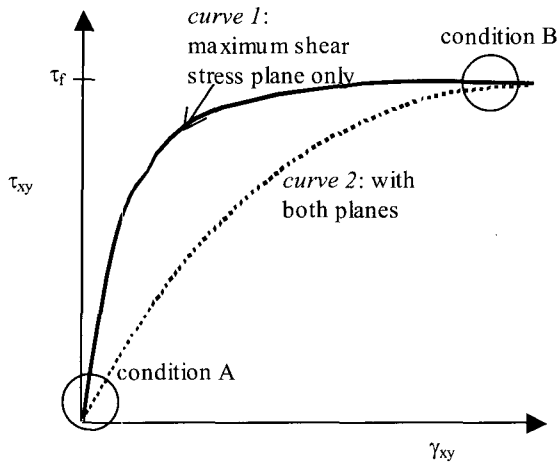


Fig. 3. Shear stress-strain curves using two mobilized planes under  $K_0$  condition

the plastic strain. This is accounted for by gradually phasing out the plastic strain increment from the horizontal plane as the plane of maximum shear becomes horizontal. This stress strain condition is depicted as condition B on Figure 3. Note that if  $K_0 = 1$  then the plane of maximum shear becomes horizontal as soon as the first increment of  $\Delta\tau_{xy}$  is applied and the horizontal plane contribution is not needed. It is depicted in Figure 2 (b).

In summary, for simple shear conditions, the predicted response from classical plasticity will be too stiff if only the plane of maximum shear is considered as depicted in Figure 3. By including the plastic strain increments from the horizontal plane a softer response in keeping with observed response is predicted. For the special case of  $K_0 = 1$ , the plane of maximum shear is approximately horizontal throughout simple shear loading, and there is no need to consider a second plane. For cyclic triaxial tests the direction of principal stress remains vertical and there is no rotation of principal stress and no need to consider a second plane. However, earthquakes induced loading conditions are much closer to simple shear than conventional triaxial loading, and it is important therefore to consider a second plane for seismic loading.

### 3.2 Elastic Behaviour

Elastic behaviour is assumed isotropic and expressed in terms of bulk and shear moduli. The elastic bulk modulus,  $B$ , and shear modulus,  $G$ , are stress level

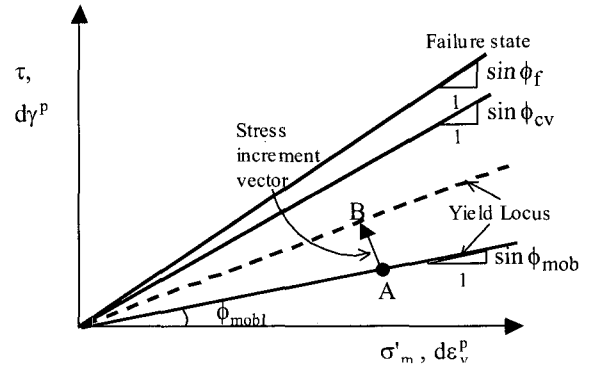


Fig. 4. Failure and yield conditions

dependent and described by the following relations, where  $K_B^e$  and  $K_G^e$  are modulus numbers,  $P_A$  is atmospheric pressure, and  $\sigma'_m$  is the mean effective stress:

$$B = K_B^e \cdot P_A \cdot \left( \frac{\sigma'_m}{P_A} \right)^{0.5} \quad (1)$$

$$G = K_G^e \cdot P_A \cdot \left( \frac{\sigma'_m}{P_A} \right)^{0.5} \quad (2)$$

### 3.3 Plastic Behaviour on Maximum Shear Stress Plane

The formulation is based on classical plasticity. Yield loci are radial lines from the origin of stress space corresponding to the mobilized friction angle. The proposed model is a Mohr-Coulomb type of model (Vermeer 1980). Since the sine of a mobilized friction angle corresponds to the ratio of shear stress to mean stress,  $\tau/\sigma'_m$ , yield loci  $f_1$  are assumed to be radial lines of constant stress ratio as shown in Figure 4 and expressed by

$$f_1 = \tau_1 - \sigma'_m \cdot \sin(\phi_{mob})_1 \quad (3)$$

where  $\tau_1$  = the maximum shear stress, and  $(\phi_{mob})_1$  = the friction angle mobilized on the maximum shear stress plane. Reloading induces plastic response but with a stiffened plastic shear modulus. The plastic shear modulus relates the shear stress and the plastic shear strain and is assumed to be hyperbolic with stress ratio as shown in Figure 5. Moving the yield locus from A to B in Figure 4 induces a plastic shear strain increment,  $d\gamma^p$ , as

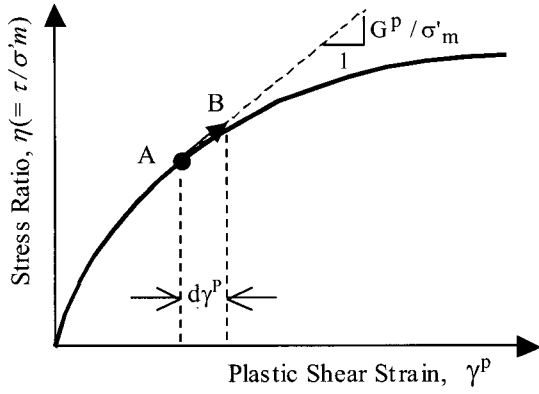


Fig. 5. Hardening rule

shown in Figure 5, and is controlled by the plastic shear modulus,  $G^P$ . The flow rule defines the direction of the plastic strain increments and is non-associated here. The plastic potential  $g_1$  used in the flow rule is a function of dilation angle as follows:

$$g_1 = \tau_1 - \sigma'_m \cdot \sin(\psi)_1 \quad (4)$$

where  $(\psi)_1$  is the dilation angle based on laboratory data and energy considerations and is approximated by

$$\sin(\psi)_1 = \sin \phi_{cv} - \sin(\phi_{mob})_1 \quad (5)$$

where  $\phi_{cv}$  is the phase transformation or constant volume friction angle and  $(\phi_{mob})_1$  describes the current yield locus. A positive value of  $\sin(\psi)_1$  corresponds to contraction. Contraction occurs for stress states below  $\phi_{cv}$  and dilation above. The associated plastic volumetric strain increment,  $d\varepsilon_v^P$ , is obtained from  $d\gamma^P$  and the dilation angle  $(\psi)_1$ :

$$d\varepsilon_v^P = d\gamma^P \cdot \sin(\psi)_1 \quad (6)$$

### 3.4 Plastic Behaviour on Horizontal Plane

Yield loci associated with the horizontal plane,  $f_2$ , have the same shape as those for the maximum shear stress plane and are expressed by

$$f_2 = \tau_2 - \sigma'_m \cdot \sin(\phi_{mob})_2 \quad (7)$$

where  $\tau_2 = \tau_{xy}$ , the shear stress acting on a horizontal

plane, and  $(\phi_{mob})_2 =$  the friction angle mobilized on a horizontal plane. The horizontal plane will contribute to both loading and unloading component. In terms of the amount of plastic strains, this contribution will be maximum when shearing starts under a  $K_0$  state. It will gradually decrease as the plane of maximum shear stress rotates. After the maximum shear stress plane becomes horizontal, the contribution from this horizontal plane becomes zero. The plastic volumetric strain increment and dilation angle are similar to those in Eq. 5 and Eq. 6. However, the dilation angle,  $\sin(\psi)_2$ , is based on a mobilized angle on a horizontal plane,  $\sin(\phi_{mob})_2$  and expressed by

$$\sin(\psi)_2 = \sin \phi_{cv} - \sin(\phi_{mob})_2 \quad (8)$$

### 3.5 Hardening Rule and Elasto-plastic Behaviour

The hardening rules are similar for both maximum shear stress and horizontal planes. The only difference is the stress ratio,  $\eta$ . The plastic properties used by the model are the peak friction angle  $\phi_p$ , the constant volume friction angle  $\phi_{cv}$ , and plastic shear modulus  $G^P$ , where

$$G^P = G_i^P \cdot \left(1 - \frac{\eta}{\eta_f} R_f\right)^2 \quad (9)$$

$G_i^P = \alpha G$  and depends on relative density,  $\eta$  ( $= \tau_1/\sigma'_m$  or  $\tau_2/\sigma'_m$ ) is the stress ratio,  $\eta_f$  is the stress ratio at failure, and  $R_f$  is the failure ratio used to truncate the hyperbolic relationship.

For loading on the plane of maximum shear, the position of the yield locus  $(\phi_{mob})_1$  is initially specified for each element. As the stress ratio increases and plastic strain is predicted, the yield locus for that element is pushed up by an amount  $d(\phi_{mob})_1$  as given by Eq. 10.

$$d(\phi_{mob})_1 = \left(\frac{G^P}{\sigma'_m}\right) \cdot d\gamma^P \quad (10)$$

Upon unloading, plastic deformation is controlled by conditions on the horizontal plane using an incremental formulation of Eq. 7 and expressed in Eq. 11. The initial yield locus is set at the stress reversal point C in Figure

6 and plastic shear strain,  $d\gamma^P$ , upon unloading is predicted based on Eq. 11 until the shear stress changes sign, or the reversal occurs.

$$df_2 = d\tau_2 - d\sigma'_m \cdot \sin(\phi_{mob})_2 - G^P \cdot d\gamma^P = 0 \quad (11)$$

During unloading and reloading, plastic shear moduli are based on modified shear stresses as given by Eq. 12 and illustrated in Figure 6, where  $\eta^* = \tau^*/\sigma'_m$  and  $\eta_f^* = \tau_f^*/\sigma'_m = (\tau_r + \tau_f)/\sigma'_m$ . Reloading then occurs with a stiffened modulus:

$$G^P = G_i^P \cdot \left(1 - \frac{\eta_f^*}{\eta_f^*} R_f\right)^2 \quad (12)$$

The plastic volumetric strain increment is obtained from Eqs. 13 and 14 through dilation angle,  $\sin(\psi)_2$ . Eq. 13 is for loading and Eq. 14 is for unloading as illustrated in Figure 7. These equations are based on stress-dilatancy theory as well as the results of drained cyclic simple shear tests, Lee (1991). His results showed that dilation angle depended on stress ratio,  $\eta$ , whether loading or unloading is occurring, but was not influenced by the initial density, normal stress, or number of cycles.

$$\frac{d\varepsilon_v^P}{|d\gamma^P|} = (\sin \phi_{cv} - \eta) = \sin(\psi)_2 \quad (13)$$

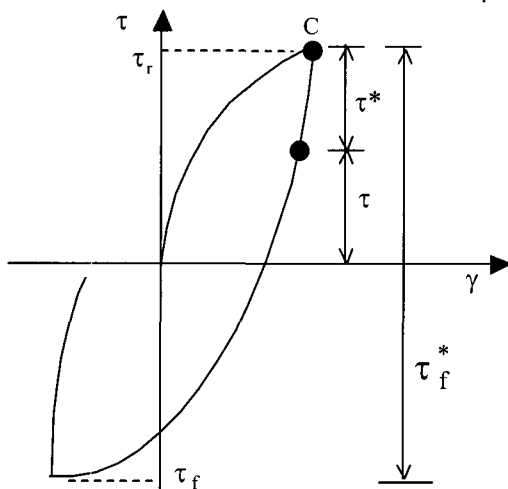


Fig. 6. Stress ratio during unloading and reloading

$$\frac{d\varepsilon_v^P}{|d\gamma^P|} = (\sin \phi_{cv} + \eta) = \sin(\psi)_2 \quad (14)$$

Plastic shear and volumetric strain increments from both the plane of maximum shear and the horizontal plane are simply added as shown in Eq. 15.

$$\left(d\varepsilon^P\right)_k = \lambda_k \cdot \frac{\partial g_k}{\partial \sigma} \quad (15)$$

where k indicates each mobilized plane causing plastic deformation (i.e.  $k = 1, 2$ ),  $\lambda$  is a scalar number, and determined by a consistency condition (i.e.  $df = 0$ ). Plastic strain increments resulting from principal stress rotation during both loading and reloading are considered on the horizontal plane. Their contribution gradually decreases as principal stresses rotate and become zero when both planes are coincident. A scalar number  $\lambda_2$  on a horizontal plane is adjusted to  $\lambda_2^*$  as follows

$$\lambda_2^* = \lambda_2 \cdot (\cos 2\alpha_\sigma)^\chi, \text{ where } 0 \leq (\cos 2\alpha_\sigma)^\chi \leq 1.0 \quad (16)$$

where  $\alpha_\sigma$  is a principal stress rotation angle from the vertical, and  $\chi$  is an adjusting parameter to give a best fit. When both planes are coincident,  $\lambda_2^* = 0$ .

The response of sand is controlled by the skeleton behaviour. A fluid (air water mix) in the pores of the sand acts as a volumetric constraint on the skeleton if drainage is curtailed. It is this constraint that causes the

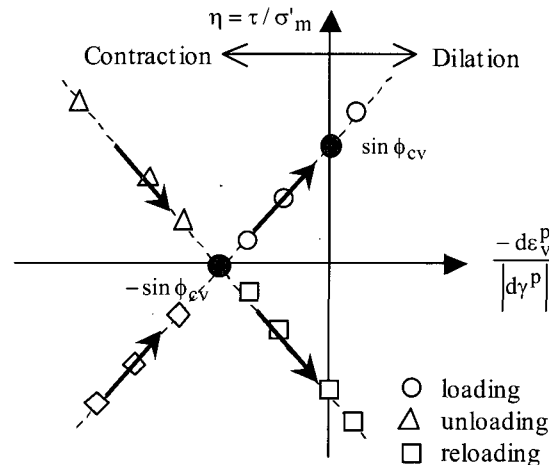


Fig. 7. Shear volume coupling

pore pressure rise that can lead to liquefaction. Provided the skeleton or drained behaviour is appropriately modeled under monotonic and cyclic loading conditions, and the stiffness of the pore fluid ( $B_f$ ) and drainage are accounted for, the liquefaction response can be predicted. This concept is incorporated in the Two Mobilized-Plane Model.

#### 4. Calibration

A series of simple shear tests were performed on Fraser River sand at UBC and used as a database to calibrate the numerical model element response. Test data are available on web site (<http://www.civil.ubc.ca/liquefaction/>). The samples were prepared by air pluviation method, which is normally adopted in centrifuge tests. The details including test results can be found in Wijewickreme et al. (2005) and Sriskandakumar (2004). Drained behaviour of the sand was first captured by the model as shown in Figure 8. The initial horizontal stress in the test was assumed to be 50 kPa, i.e.,  $K_0 = 0.5$ . The elastic and plastic parameters selected for calibration were approximated from UBCSAND model and adjusted to match drained response as listed in Table 1.

Two numerical predictions with the same initial mean stress for the test (Relative density at the end of con-

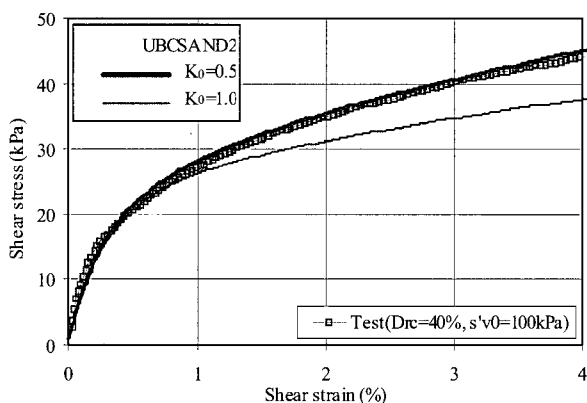


Fig. 8. Numerical simulations of  $K_0=0.5$  and  $1.0$  with the same initial mean stress

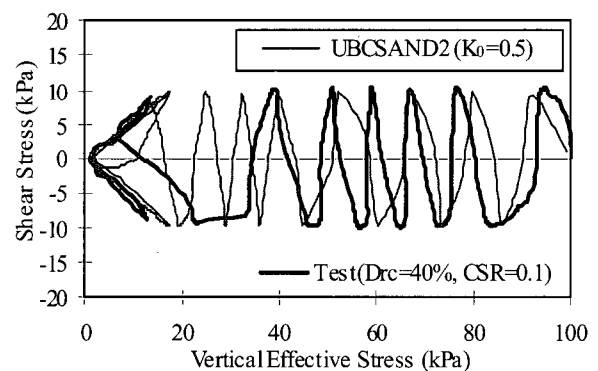
Table 1. Input parameters for  $D_{rc} = 40\%$  Fraser River sand

Parameters	$K_0^e$	$K_{Be}$	$\alpha$	$\phi_{cv}$	$\eta_t$	$R_t$
Values	622	249	0.4	33	0.58	0.99

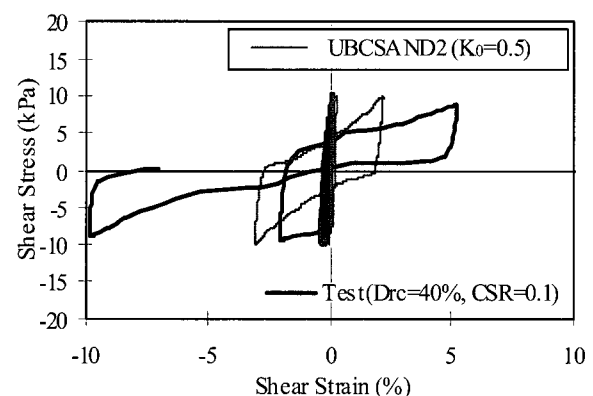
solidation  $D_{rc} = 40\%$  and  $\sigma'_{v0} = 100$  kPa) give similar response at small shear strain ( $\gamma < 1\%$ ), regardless of  $K_0$  conditions. Upon further shearing, the  $K_0 = 0.5$  case (thick line) gives a stiffer response because the horizontal stress rises and increases  $\sigma'_m$ .

Samples were also subjected to cyclic shear for a range of cyclic stress ratios under constant volume conditions that simulate undrained response. Tests were carried out for four different CSRs (Cyclic Stress Ratio), 0.08, 0.1, 0.12 and 0.15. Typical results of measured response of  $D_{rc} = 40\%$  for  $CSR = 0.1$  are shown in Figures 9 (a) and 9 (b). Test data are shown as the heavy lines. The thin lines are the numerical predictions for  $K_0 = 0.5$ . When  $CSR = 0.1$ , liquefaction occurred in 6 cycles. It is observed that the first and last cycles generated large excess pore pressures. Once the pore pressure ratio reached unity, large cyclic strains developed referred to as cyclic mobility.

The CSR versus number of cycles to liquefaction is



(a) Predicted stress path under  $K_0 = 0.5$  and test result



(b) Predicted stress-strain curve under  $K_0 = 0.5$  and test result

Fig. 9

shown in Figure 10. Liquefaction triggering was defined as  $\gamma > 3.75\%$ , and at this point  $R_u$  (pore pressure ratio) is 90 - 95%. This strain level is equivalent to reaching a 2.5% single-amplitude axial strain in a triaxial sample, which also is a definition for liquefaction previously suggested by the National Research Council of United States (NRC 1985).

The calibration was carried out in the same way as the tests, i.e. under constant volume. The test sample was subjected to an initial vertical stress of 100 kPa under  $K_0$  conditions. It was assumed that the initial horizontal stress in the test was 50 kPa, i.e.,  $K_0 = 0.5$ . The same initial stresses were assumed in the numerical simulation. A single element was used. The input parameters selected for calibration were the same for all cases having the same  $D_{rc}$  and tabulated in Table 1. The predicted stress-strain and stress paths for  $K_0 = 0.5$  and  $CSR = 0.1$  are shown in Figures 9 (a) and 9 (b) as "thin" lines. The predictions

generally give a reasonable representation of the observed response including plastic unloading, sudden drop of effective stress during stress reversal after dilation, and cyclic mobility.

If test condition were  $K_0 = 0.5$ , the predicted triggering of liquefaction shows a good agreement with measurements as shown in Figure 10.

An examination of the effect of  $K_0$  on prediction of liquefaction resistance is shown in Figure 11. The  $K_0 = 0.5$  case had initial stresses of 100 kPa and 50 kPa, and thus a mean stress of 75 kPa. The  $K_0 = 1.0$  case had stresses of 75 kPa, and thus a mean stress of 75 kPa also. The predicted results show that both  $K_0 = 0.5$  and  $K_0 = 1.0$  states liquefaction in about the same number of cycles. This is in agreement with the test results of Ishihara (1996) who found that samples at the same density and mean stress had similar liquefaction response.

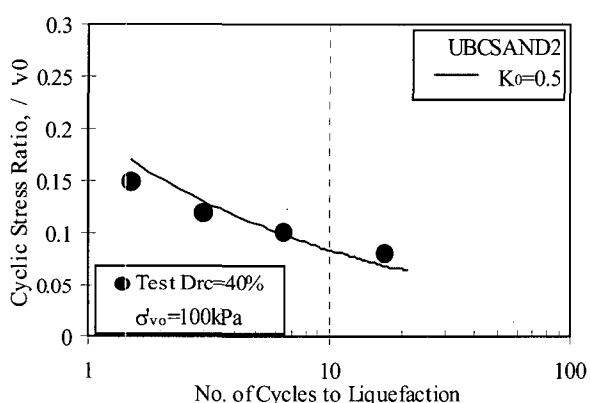


Fig. 10. Predicted liquefaction resistance under  $K_0 = 0.5$  and test result in terms of  $\tau/\sigma'_{v0}$

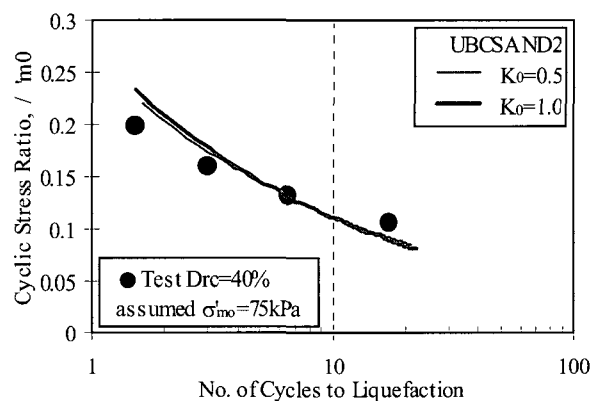


Fig. 11. Predicted liquefaction resistance in terms of  $\tau/\sigma'_{m0}$  under  $K_0 = 0.5$  and 1.0 and test result

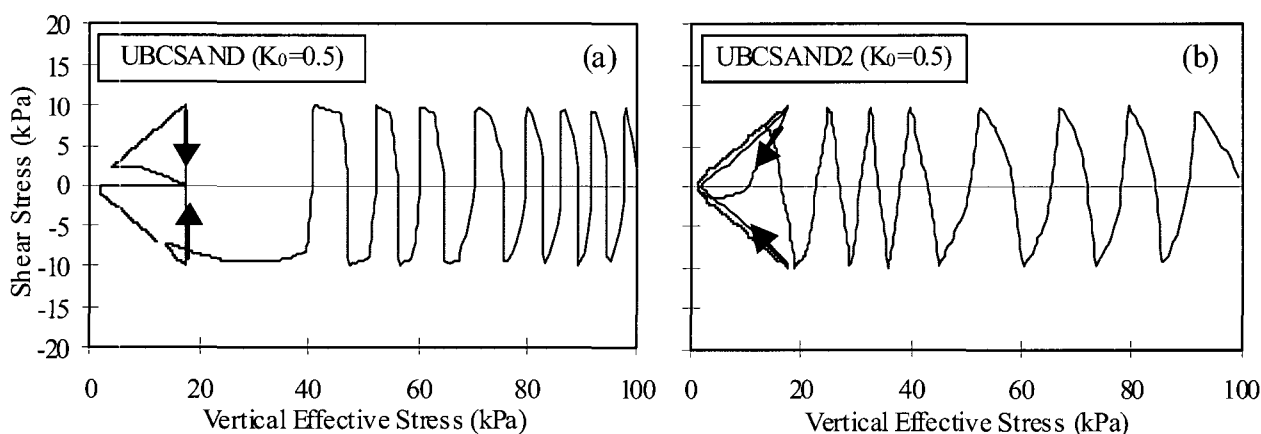


Fig. 12. Comparison of undrained stress paths using (a) UBCSAND and (b) UBCSAND2



The performance of Two Mobilized-Plane Model (UBCSAND2) is compared with UBCSAND in Figure 12. The assumption of  $K_0 = 0.5$  and input parameters used in the prediction with the Two Mobilized-Plane Model were also used in the prediction undertaken employing UBCSAND. It becomes clear that UBCSAND is not able to compute plastic deformation (e.g., plastic volume change) during the unloading phase, as indicated by straight-downward arrows in Figures 12 (a).

## 5. Conclusion

A Two Mobilized-Plane Model for predicting the stress-strain response of sand under monotonic as well as cyclic loading conditions is presented. The model is focused on simple shear loading conditions, as this is most representative of seismic loading conditions in the field. The proposed model addressed two key features; rotation of principal planes and plastic unloading. It uses two mobilized planes; a maximum shear stress plane, and a horizontal plane. The model was calibrated based on drained and constant volume simple shear tests and showed the same characteristic response as observed in the laboratory tests. The model captured the large soil compaction effect during stress reversal after dilation and general cyclic soil behaviour including cyclic mobility after triggering of liquefaction. The model also predicts that elements having the same initial density and mean stress will have similar liquefaction response, in agreement with laboratory element tests.

## Acknowledgments

The Author acknowledges that a series of simple shear tests for numerical model validation presented herein were carried out by Mr. Sriskandakumar during his MAsC studies at the University of British Columbia under the supervision of Dr. Wijewickreme at UBC. The author also acknowledges NSERC support through grant No. 246394, without which this work would not have been possible.

This work was supported by the Brain Korea 21

Project in 2006.

## References

1. Arthur, J. R. F., Chua, K. S., Dunstan, T. and Rodriguez del C. J. I. (1980), "Principal stress rotation: a missing parameter", *Journal of the Geotechnical Engineering Division*, 106(GT4), pp.419-433.
2. Iai, S., Matsunaga, Y., and Kameoka, T. (1992), "Analysis of undrained cyclic behavior of sand under anisotropic consolidation", *Soils and Foundations*, 32(2), pp.16-20.
3. Ishihara, K. (1996), *Soil behaviour in earthquake Geotechnics*, Clarendon Press, Oxford.
4. Itasca (2000), FLAC, version 4.0. Itasca Consulting Group Inc., Minneapolis.
5. Kabilamany, K., and Ishihara, K. (1991), "Cyclic behaviour of sand by the multiple shear mechanism model", *Soil Dynamics and Earthquake Engineering*, 10(2), pp.74-83.
6. Kolymbas, D. (2000), The misery of constitutive modeling, *Constitutive modelling of granular materials*, Edited by Dimitrios Kolymbas, pp.11-24.
7. Lee, C.- J. (1991), "Deformation of sand under cyclic simple shear loading", *Proceedings of the Second International Conference on Recent Advances in Geotechnical Earthquake Engineering and Soil Dynamics*, March 11-15, St. Louis, Missouri, 1, pp.33-36.
8. Lee, K.-H. and Pande, G. N. (2004), "Development of a two-surface model in the Multilaminate framework", *Proceedings of the 11<sup>th</sup> Conference on Numerical Models in Geomechanics*, Ottawa, pp.139-144.
9. Matsuoka, H. (1974), "Stress-strain relationships of sands based on the mobilized plane", *Soils and Foundations*, 14(2), pp.47-61.
10. NRC. (1985), *Liquefaction of soils during earthquakes*, National Research Council Report CETS-EE-001, National Academic Press, Washington, D.C.
11. Pande, G. N., and Sharma, K. G. (1983), "Multi-laminate model of clays-a numerical evaluation of the influence of rotation of the principal stress axes", *Int. Journal for Numerical and Analytical Methods in Geomechanics*, 7, pp.397-418.
12. Roscoe, K.H. (1970), "10<sup>th</sup> Rankine Lecture: The influence of strains in soil mechanics", *Geotechnique*, 20, pp.129-170.
13. Sriskandakumar, S. (2004), *Cyclic loading response of Fraser River sand for validation of numerical models simulating centrifuge tests*, MAsC Thesis, Department of Civil Engineering, UBC.
14. Vermeer, P. A. (1980), "Formulation and analysis of sand deformation problems", Report 195 of the Geotechnical Laboratory, 142p. Delft University of Technology.
15. Wijewickreme, D. and Vaid, Y. P. (2004), "A descriptive framework for the drained response of sands under simultaneous increase in stress ratio and rotation of principal stresses", Submitted to *Soils and Foundations*.
16. Wijewickreme, D., Sriskandakumar, S., and Byrne, P.M. (2005), "Cyclic Loading Response of Loose Air-pluviated Fraser River Sand for Validation of Numerical Models Simulating Centrifuge Tests", *Canadian Geotechnical Journal*, 42(3), pp.550-561.

(received on Oct. 1, 2006, accepted on Oct. 24, 2006)